Theoret. Chim. Acta (Berl.) 51, 11–35 (1979)

THEORETICA CHIMICA ACTA

A Theoretical *ab initio* Study of the Reaction of Formation of 2-Fluoroethanol from Oxirane and HF

Giuliano Alagona, Eolo Scrocco and Jacopo Tomasi

Laboratorio di Chimica Quantistica ed Energetica Molecolare del C.N.R., Via Risorgimento, 35, I-56100 Pisa, Italy

The reaction of ring opening of epoxides under the action of a halogenic acid has been investigated using as model the system $C_2H_4O + HF \rightarrow CH_2OHCH_2F$. The physical conditions chosen for the model more directly correspond to the gas phase reaction and under these conditions the preferred mechanism leads to the formation of a halohydrine having the same configuration at the C atom as the reagent.

Parallel investigations have been performed on other mechanisms which postulate the preliminary formation of the conjugate acid of the oxirane ($C_2H_4OH^+$) and proceed via the well known mechanisms A_1 or A_2. In this case the best mechanism corresponds to the so-called "borderline A_2" mechanism. This last type of mechanism probably is the dominant one in protic solutions, but by coupling the present calculations with experimental conductometric measurements in anhydrous aprotic media one could consider the first concerted mechanism as a possible candidate also for the reaction in "inert" media.

A qualitative analysis of the transition state indicates, in addition, that the propension for the retention path, is probably emphasized by the use of HF as reactant, and that with other acids, like HCl, or even by assuming the presence of dimers like HF·HF, the inversion path could be preferred.

The investigations have been done by determining the geometry of the transition state and the reaction coordinate with *ab initio* SCF STO-3G calculations on the whole nuclear configuration space (21 dimensions). These calculations have been supplemented by a few CI calculations on the same basis set and by a few SCF calculations with a larger basis set.

Key words: Ring opening reactions for epoxides – Oxirane-HF reaction mechanism

0040–5744/79/0051/0011/$05.00

1. Introduction

The main subject of this paper is a theoretical investigation on the mechanism of the formation of halohydrines from epoxides and halogenic acid. This study has been performed on a physical model consisting of only one molecule of epoxide and one molecule of halogenic acid which corresponds, *stricto sensu*, to the situation one can find in low pressure gas phase reactions. The reader could ask why we have selected for this investigation physical conditions not yet met in practice for a reaction which is well known and of considerable interest in solution. The reason which has prompted us to undertake the present investigation has been the experimental evidence, obtained via conductometric measurements performed in our laboratory[1], that in anhydrous non-polar solvents the reaction can proceed without an appreciable concentration of ionic conducting species being present in the solution.

The large amount of literature on this reaction mechanism agrees in assuming as a first step in the reaction the rapid formation of the conjugated acid of the epoxide:

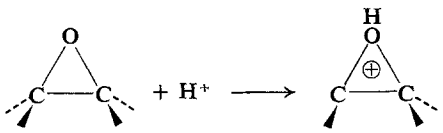

(1)

while the discussion concerns the following step of the reaction, which could proceed according to one of the following two mechanisms A_1 or A_2

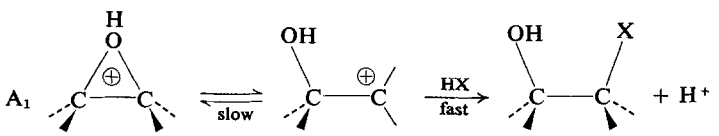

(2)

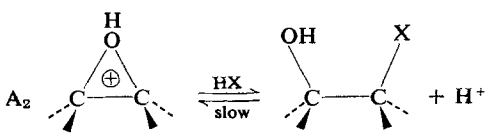

(3)

or according to other related mechanisms as the "borderline A_2" one [1–9]. (We have not considered here other possible steps involving solvolysis, which can be safely discarded in aprotic media.) These descriptions of the whole mechanism require the presence of ionic species. The main aim of this paper thus consists in checking whether or not there is the possibility of getting the halohydrine without invoking a previous protonation of the epoxide, i.e. a previous heterolytic scission of the HX molecule. To save computing time we have selected for this study the simplest epoxide, oxirane, and the simplest halogenic acid, HF.

---

[1] Under the same experimental conditions as the relevant reaction (epoxide $\simeq 0.02N$ and HCl $\simeq 0.02N$ in CCl_4 or toluene) the specific conductivities measured were about $10^{-10}\ \Omega^{-1}\ cm^{-1}$. Even if this quantity refers to a very low ionic concentration, we cannot *a priori* exclude that, in non-polar solvents, the reaction can proceed with an ionic mechanism in consequence of its low activation energy.

Previous theoretical investigations on the opening reactions of three-membered cycles have been especially related to mechanisms which do not involve a second reactant; the bulk of these investigations regards the cyclopropane ring but there are also a few *ab initio* studies which consider the C—C [10, 11] and C—O [12] bond disruption in oxirane. To the best of our knowledge bimolecular ring opening reactions of oxirane have been theoretically studied only in two papers [13, 14]: in the first the reactant is H^- and the study looks essentially at the early stage of the reaction preceding the transition state; in the second the reactant is the protonated oxirane and the reaction does not present an energy barrier. Both studies have been performed with semiempirical methods. Since the completion of the present work a paper by Hopkinson *et al.* [15] on the reaction between ethylene and OH^+ which covers some aspects of the ring opening mechanism of the protonated oxirane has been published. The number of theoretical investigations on the interaction of oxirane with a proton [16–19] or with other small molecules or ions [20–22] is larger but they concern the formation of adducts where the cyclic structure of oxirane is maintained.

2. Basic Outline of the Investigation and Computational Details

The main portion of this paper regards an *ab initio* determination of the reaction coordinate connecting the reagents (C_2H_4O + HF) to the products ($HOCH_2CH_2F$). Particular attention has been paid to the examination of competitive paths leading to inversion or to retention of configuration of the C atom which at the end of the reaction will bear the halogen. The number of independent geometrical parameters in this molecular system is 21; an independent optimization of practically all the values assumed by these parameters has been found to be necessary in several regions of the hypersurface. More detailed information on the optimization strategies we have adopted will be given in the course of the paper.

This description of the bimolecular reaction mechanism has been obtained via SCF calculations with the STO-3G basis set, supplemented by a few CI calculations on the same basis set and by SCF calculations on a larger basis (4-31G).

In addition we report some results of parallel investigations on the opening of protonated oxirane (see mechanism A_1, scheme 2), of the reaction of protonated oxirane with HF (see mechanism A_2, scheme 3) or with F^-, and of the opening of neutral oxirane without the intervention of other agents. In the following account we shall consider separately the following points: (1) identification of the initial and final products, (2) non-covalent interactions between oxirane and HF, (3) comparative examination of the ring opening energy profile in neutral oxirane, in the $C_2H_4O \cdot HF$ complex, and in $C_2H_4OH^+$, (4) the reaction mechanism of formation of 2-fluoroethanol starting from $C_2H_4OH^+$, (5) a description of the best paths available for a bimolecular mechanism of formation of $HOCH_2CH_2F$ starting from oxirane and HF.

3. Characterization of the Initial and Final Products

The optimum geometry of oxirane in the STO-3G basis set was published some years ago by Pople and coworkers [23]. Our geometry optimization was performed

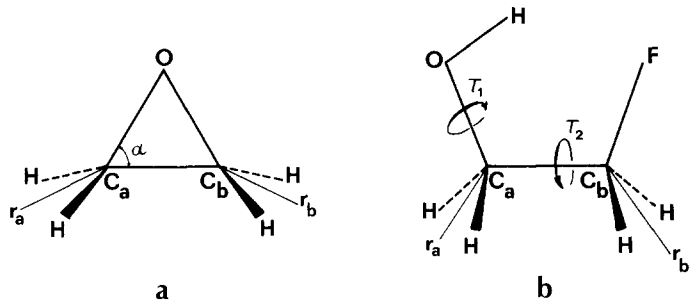

Fig. 1. Notation of the geometrical parameters of oxirane (a) and 2-fluoroethanol (b)

without a previous knowledge of this paper, and the comparison between the two sets of results can be considered as a check of our geometry optimization programme which follows a strategy of iterative independent optimizations of every geometrical parameter with the selection, at every step, of the parameter showing the largest energy decrease. The values we have obtained agree with those of Pople and coworkers to all decimal digits given. There is also a more recent independent geometry optimization with the STO-3G basis set [19]; this new set of values presents only minor differences with respect to the preceding one (and also the total energy is higher by only 0.03 kcal/mole) so that we may state that this geometry has

Table 1. Optimum geometry parameters of oxirane at the equilibrium geometry and at an open form having $O\widehat{C_aC_b} = 90°$

	A	B
Distances, Å		
C_aC_b	1.483	1.406
C_aO	1.433	1.380
C_aH	1.088	1.088
C_bH	1.088	1.088
Angles, deg		
$O\widehat{C_aC_b}$	58.84	*90*[b]
$H\widehat{C_aH}$	114.5	108.0
$H\widehat{C_bH}$	114.5	116.8
$r_a\widehat{C_aC_b}$	155.3	136.2
$C_a\widehat{C_br_b}$	155.3	194.5
ρ_b[a]	0	0
E, hartrees	−150.9285	−150.7958
ΔE, kcal/mole	0	83.3

[a] ρ_b measures the rocking motion of C_bH_2 (rotation of that group with respect to the C_a—C_b axis, with positive values corresponding to clockwise rotations).

[b] The value in italics is not optimized.

been independently checked by three groups. In Fig. 1a we give the notation of the geometry parameters employed in this paper and in Table 1 the corresponding numerical values.

To the best of our knowledge there is not a complete geometry optimization of 2-fluoroethanol with the STO-3G basis set (a partial optimization has been done in Ref. [24]). Fig. 1b shows the geometrical parameters we have adopted and Table 2 contains the corresponding numerical values. This geometry agrees fairly well with the experimental results obtained by different researchers with different techniques ([24, 25] and Refs. quoted therein).

The fluoroethanol has two rotational parameters (τ_1, τ_2). The most stable conformation nearly corresponds to (−60, 60), i.e. to the $g'G$ conformation according to the notation of Radom *et al.* [27] who performed an investigation on the rotational

Table 2. Optimum geometry of 2-fluoroethanol at two different conformations and its changes due to the closure of the α angle

	A	B	C	D
Distances, Å				
C_aC_b	1.558	1.553	1.588	1.685
C_aO	1.433	1.437	1.476	1.545
OH	0.991	0.991	0.991	0.991
C_bF	1.387	1.387	1.389	1.387
C_aH	1.095	1.097	1.093	1.087
C_bH	1.098	1.098	1.097	1.098
Angles, deg				
$\widehat{HOC_a}$	103.49	103.09	104.74	104.60
$\widehat{OC_aC_b}$	112.25	107.83	*90*[c]	*70*
$\widehat{HC_aH}$	107.94	107.58	111.58	116.24
$\widehat{HC_bH}$	108.18	107.82	107.92	104.50
$\widehat{C_aC_bF}$	110.0	110.27	109.21	106.22
$\widehat{r_aC_aC_b}$	123.35	123.44	133.14	149.06
$\widehat{C_aC_br_b}$	124.71	124.12	125.74	129.21
τ_1[a]	−57.37	*180*	180	180
τ_2[a]	62.53	*180*	180	180
ρ_a[b]	2.55	0	0	0
E, hartrees	−249.5801	−249.5785	−249.5599	−249.4670
ΔE, kcal/mole	0	1.0	12.7	70.9

[a] τ_1 = torsional angle C_bC_aOH; τ_2 = torsional angle OC_aC_bF. These torsions measure the rotation of the OH and CH_2F groups respectively. The torsion angle of the system ABCD is defined as the angle between the planes ABC and BCD; this angle is positive for clockwise rotations of CD around BC when looking from B to C. The reference conformation is given in Fig. 1b.

[b] ρ_a measures the rocking motion of C_aH_2 (rotation of that group with respect to the C_a–C_b axis, with positive values corresponding to clockwise rotations).

[c] The values in italics are not optimized.

Table 3. Conformational energies of 2-fluoroethanol. (Relative values in kcal/mole.)

(τ_1, τ_2)	A	B	C	D	E
$(-60, 60)$ $g'G$	0	0	0	0	0
$(60, 60)$ gG	4.13	1.40	1.35	1.63	1.49
$(180, 60)$ tG	3.15	0.96	1.83	0.35	1.07
$(60, 180)$ gT	2.01	1.34	1.26	1.36	1.31
$(180, 180)$ tT	0.76	0.64	1.55	−0.03	0.75

A. 4-31G calculations with standard bond lengths and angles: $E_{g'G} = -252.58044$ hartrees
B. STO-3G calculations with standard bond lengths and angles: $E_{g'G} = -249.57507$
C. STO-3G calculations on the structure $g'G$ with $\rho_a = 0°$: $E_{g'G} = -249.57973$
D. STO-3G calculations on the structure tT: $E_{g'G} = -249.57848$
E. STO-3G calculations with intermediate values: $E_{g'G} = -249.57942$

conformers of these molecules using a 4-31G basis and standard values for bond lengths and angles. This conformation is stabilized by the formation of an intramolecular hydrogen bond involving the F atom and the OH group.

It may be of some interest to examine how the rotational energy surface depends on the values of the other geometrical parameters. We give in Table 3 the relative value of a few selected conformers calculated (A) with the 4-31G basis set at standard values of the other parameters (energies taken from Ref. [27]), (B) with the STO-3G basis set and the same values as above of the other parameters, (C) with the STO-3G basis set and internal parameters kept fixed at the best values found for the $(-60, 60)$ conformation, (D) with the same basis set and internal parameters kept fixed at the best values found for the (180, 180) conformation, (E) with values of the internal parameters which constitute a compromise between the values found by optimization at the $(-60, 60)$ and (180, 180) conformations.

The changes in the rotational surface produced by a change of basis agree with those found in previous investigations [28]; the energy differences are overestimated by the 4-31G basis and probably underestimated by the STO-3G one. The use of internal parameters optimized at a single conformation introduces serious deformations in the form of the energy surface (compare columns C and D of Table 3). The optimal geometry of the (180, 180) conformation is reported in Table 2 (column B): the largest difference with respect to the parameters of the $(-60, 60)$ conformation (which are not reported, being practically equal to those given in column A of Table 2) is for the $\widehat{CC_aC_b}$ angle. The value adopted for this angle influences the relative stability of conformations having different τ_1 values. Rather critical also is the value assumed by ρ_a (i.e. the angle defining the rocking of the C_aH_2 group); this torsion is in general quite small (less than 3°) but produces changes in the relative energies of the conformers of the order of 0.5 kcal/mole.

Experimentally [26] the difference between the G and T conformations is of the order of 2 kcal/mole; the STO-3G basis set, with complete optimization of the

parameters, gives a difference of 1.0 kcal/mole. The parameters adopted in the last column of Table 3, though being quite different from the standard ones, give a description of the rotational surface in remarkably good agreement with that reported in column B.

In the SCF STO-3G approximation the energy difference between C_2H_4O + HF and CH_2OHCH_2F is −49.4 kcal/mole, and with the 4-31G basis is −43.1 kcal/mole. Experimentally the reaction heat at 298°K is −21.5 kcal/mole[2], and the difference of energy measured from the bottom of the potential energy curves is −25 kcal/mole.

4. Non-Covalent Interactions between Oxirane and HF

The most stable complex between oxirane and HF is a hydrogen-bonded adduct where O acts as proton acceptor. Geometry optimization of this complex shows

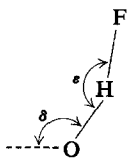

(4)

that HF lies on the perpendicular symmetry plane of C_2H_4O. The best values for two conformational angles (see scheme 4): $\delta = 128.1°$ and $\varepsilon = 174°$ indicate that the hydrogen bond deviates slightly from linearity and that its orientation does not greatly differ from that found for the oxirane-water H bond [20]. The value of the O—H distance (1.76 Å) and the stabilization energy of the complex (−4.9 kcal/mole) are in line with the values found with the same basis set for analogous complexes. It must be added that for a wide range of δ and ε values (at $R_{OH} \simeq 1.8$ Å) the stabilization energy remains practically constant. Less favoured are the conformations having HF on the ring plane (the best energy we have found with this constraint is −1.5 kcal/mole). Geometry optimization does not alter the internal geometry of C_2H_4O; the optimum geometry of $C_2H_4O \cdot HF$ complex is given in column A of Table 4.

Complexes where HF acts as a proton acceptor are less stable. At its best geometry the complex involving a CH_2 group has the F—H molecule nearly colinear with a C—H bond; the C—F distance in C—H···F is 3.3 Å and the stabilization energy is −0.7 kcal/mole. This complex is more stable by 0.4 kcal/mole of the bifurcated one which involves both C—H bonds in the interaction.

5. Comparative Examination of the Ring Opening Energy Profile in Different Limit Cases

The internal geometrical parameter most suitable to follow the ring opening mechanism in oxirane and related compounds is the $\widehat{OC_aC_b}$ angle which we shall

[2] The data for oxirane and HF are taken from the JANAF tables [29], for 2-fluoroethanol from the NBS tables [30] and from Wyn-Jones and Orville-Thomas [31].

Table 4. Optimum geometry of the adduct $C_2H_4O \cdot HF$ at the equilibrium and at different values of the $\widehat{OC_aC_b}$ angle

	A	B	C
Distances, Å			
C_aC_b	1.483	1.415	1.391
C_aO	1.433	1.386	1.390
OH	1.763	1.754	1.743
HF	0.955	0.955	0.955
C_aH	1.088	1.088	1.090
C_bH	1.088	1.085	1.085
Angles, deg			
$\widehat{FHO}$	173.9	174.0	173.8
$\widehat{HOC_a}$	121.9	119.8	117.2
$\widehat{OC_aC_b}$	58.8_5	*70*[c]	*90*
$\widehat{HC_aH}$	114.7	110.8	108.0
$\widehat{HC_bH}$	114.7	116.9	117.6
$\widehat{r_aC_aC_b}$	155.7	149.0	139.4
$\widehat{C_aC_br_b}$	155.7	165.6	187.4
τ_1[a]	−112.1	−104.0	−79.9
ρ_a[a]	0.15	0.15	0.21
ρ_b[a]	0.15	0	0
τ_3[b]	37.5	21.7	24.3
E, hartrees	−249.50923	−249.48001	−249.37846
ΔE, kcal/mole	0	18.3	82.1

[a] For its definition see Table 1 and Table 2.

[b] τ_3 = torsional angle C_aOHF. This angle measures the rotation of the HF group. In the reference conformation the H and F atoms are on the ring plane and the F and C_a atoms are in *cis* position.

[c] The values in italics are not optimized.

call α for brevity. In this section we shall compare the energy profile for changes of α with simultaneous optimization of all the other parameters, in three limiting cases, which will be useful for a better evaluation of the characteristics of the mechanism which we are looking for. The three cases are: oxirane alone, the H bonded complex of oxirane-HF, the protonated oxirane $C_2H_4OH^+$.

5.1. The Ring Opening Mechanism in Oxirane

The energy increases smoothly for increasing values of α (see Fig. 2). It may be of some interest to look at the variation of the internal geometrical parameters induced by this enlargement of α. We report in Table 1 the geometry found for $\alpha = 90°$.

The most remarkable change is a shortening of the C—C and C_a—O bond lengths; analogous changes have been found also in the open form of oxirane obtained by breaking the C—C bond. Of some interest for our specific problem are the motions

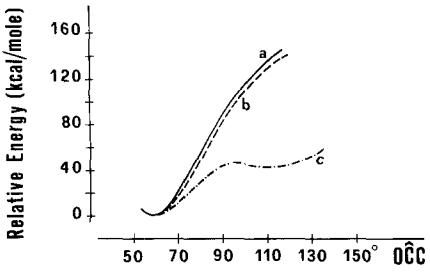

Fig. 2. Energy variation for the opening of the α angle in oxirane (curve a), oxirane-HF adduct (curve b) and oxiranium ion $C_2H_4OH^+$ (curve c). The three curves are optimized in all the other geometrical parameters

of the C_bH_2 group induced by this opening of the α angle. The orientation of C_bH_2 with respect to the molecular remainder ($\widehat{C_aC_br_b} = 194.5°$, $\rho_b = 0°$) has been obtained by inversion at the C_b atom rather than by rotation of the whole CH_2 group (when α changes from 58.8° to 90°, ρ_b remains equal to 0°). As we shall see later a direct attack of HF on a deformed oxirane having $\alpha \simeq 90°$ can lead to the formation of a fluoridine with inversion of configuration.

It must be added that the energy profile for the rotation of CH_2 around the C—C axis is not well reproduced by SCF calculations, which overestimate this barrier. In fact a closed-shell description of the system during this rotation is not sufficient. A reasonable description of the energy curves for rotational motions in systems having a non-negligible diradicalic character can be obtained [32] by adopting the half-electron effective Hamiltonian [33–35] supplemented by a 3×3 CI calculation [36, 37] involving the configurations (i^2), (ij) and (j^2) where i and j are the highest occupied and the lowest empty orbitals in the half-electron Hamiltonian approximation (and in the SCF description too).

The rotational barrier in the S_0 state (we note, in passing, that at $\alpha = 90°$ the lowest electronic state is a triplet, see also Mezey *et al.* [12]) turns out to be, in this approximation, of the order of 32.8 kcal/mole, a value decidedly more reasonable than the values of 98.6 kcal/mole obtainable with the SCF one-determinant approximation. The reason for this difference in the rotational barrier can be found in the different weight the different conformations have at different torsional angles; at $\rho_b = 0°$ the (i^2) configuration gives the main contribution to the wavefunction, while at $\rho_b = 90°$ the electronic distribution could be satisfactorily described by the (ij) configuration alone. It may be added that at larger values of the α angle this rotational barrier decreases; at $\alpha = 105°$ the rotation in the 3×3 CI approximation is practically free. (In the SCF description it remains of the order of 100 kcal/mole.)

5.2. The Ring Opening Mechanism in the $C_2H_4O \cdot HF$ *Adduct*

Curve *b* in Fig. 2 gives the energy profile for the ring opening reaction of the adduct. To make more evident the effect of complexation on the energy rise when the α angle is opened, we have adopted for both curves the same zero of energy at $\alpha = 58.8°$.

The changes of the internal geometry of the complex at various α values are more or less in line with the analogous changes in oxirane (some results are given in

Table 5. Gross group charges[a] of some selected geometries of oxirane, oxirane-HF adduct and oxiranium ion

	C_2H_4O		$C_2H_4O \cdot HF$		$C_2H_4OH^+$		
α	58.84	90	58.85	90	59.84	90	100
C_bH_2	0.104	0.108	0.129	0.143	0.396	0.608	0.694
C_aH_2	0.104	0.092	0.129	0.122	0.396	0.317	0.313
O	−0.208	−0.200	—	—	—	—	—
OHF	—	—	−0.258	−0.265	—	—	—
OH	—	—	—	—	0.209	0.075	−0.008

[a] Measured in e units (1e = 4.80298×10^{-10} e.s.u.).

Table 5). For the rotational barrier of the C_bH_2 group we have a situation very similar to that described in the preceding case. The largest differences are in the electronic distribution (we give in Table 5 the group charges for a few representative cases). In passing from $\alpha \simeq 59°$ to $\alpha = 90°$ the C_bH_2 group loses 0.004 electrons in oxirane and 0.014 electrons in the complex.

The interaction of HF with oxirane produces a remarkable lowering of the energy necessary to break the F—H bond. With the STO-3G basis set the energy required for the heterolytic cleavage of HF alone is 602 kcal/mole, and it decreases to 375 kcal/mole for the cleavage of this bond in the adduct. The opening of the ring further reduces this energy: at $\alpha = 110°$ it is of the order of 288 kcal/mole. The STO-3G basis set of course greatly exaggerates the value of such dissociation energies; more reasonable predictions can be made with 4-31G calculations (which give for the cleavage of HX molecules absolute errors of the order of 20–30 kcal/mole and relative errors of the order of 10–15 kcal/mole [38]). The values given by this basis for the dissociation energy of the F—H bond are 370 kcal/mole in HF and 210 kcal/mole in $C_2H_4O \cdot HF$ at $\alpha = 59°$.

5.3. The Ring Opening Mechanism in $C_2H_4OH^+$

This mechanism has been postulated as one of the possible mechanisms governing the formation of halohydrines (mechanism A_1, see scheme 2).

We will not dwell here on a discussion of the energy balance of mechanisms which could permit the formation of "free" H^+ ions in inert anhydrous solutions of HF, however if the free proton is present, the ring opening mechanism permits the achievement (after an energy barrier) of a secondary minimum on the potential energy hypersurface (see curve c of Fig. 2).

H^+ clearly prefers to attack oxirane in the O region of the ring [17, 18]. The $C_2H_4OH^+$ species corresponds to a stable intermediate, whose optimal geometry is given in Table 6. An independent optimization performed by Catalán and Yáñez [19] with the same basis set presents some small differences which, as we have

Table 6. Optimized geometries for $C_2H_4OH^+$

	A	B	C
Distances, Å			
C_aC_b	1.496	1.515	1.540
C_aO	1.488	1.436	1.430
OH	1.010	0.995	0.991
C_aH	1.095	1.096	1.108
C_bH	1.095	1.110	1.116
Angles, deg			
$\widehat{HOC_a}$	114.28	106.0	105.0
$\widehat{OC_aC_b}$	59.84	*90*[b]	*110*
$\widehat{HC_aH}$	117.6	111.7	106.9
$\widehat{HC_bH}$	117.6	117.0	118.4
$\widehat{r_aC_aC_b}$	162.6	125.6	123.4
$\widehat{C_aC_br_b}$	162.6	191.2	179.9
τ_1[a]	−105.20	−104.30	180
ρ_a[a]	2.0	2.6	0
ρ_b[a]	2.0	0	90
E, hartrees	−151.2982	−151.2301	−151.2290
ΔE, kcal/mole	0	42.7	43.4

[a] For its definition see Tables 1 and 2.
[b] The values in italics are not optimized.

observed in the case of the neutral molecule, are not of practical importance. For a discussion about the geometry changes produced by the protonation we may make reference to that paper.

The opening of the ring, via the enlargement of the α angle, requires a decidedly lower energy with respect to the two preceding cases. We give the energy profile in Fig. 2 (curve c). In this case too we have shifted the energy curve to make the three curves coincident at $\alpha = 58.8°$.

The minimum at $\alpha \simeq 110°$ actually corresponds to a true relative minimum; the geometrical parameters, together with the best ones obtained at $\alpha = 90°$, are given in Table 6. The ring opening corresponds to a lengthening of the C—C bond and a shortening of the C—O bond. There is a remarkable shift of the charge density (see Table 5): in the cyclic form the formal +1 charge is accounted for only by 20% from the OH group, at $\alpha = 100°$ the OH group is practically neutral (with a noticeable local dipole moment, the formal charges of H and O being respectively +0.245 and −0.253 e) and the charge shift mainly concerns the C_bH_2 group which assumes the characteristics of a $\diagdown\!\!\diagup CH_2^+$ group. The conformation of the OH bond is *trans* with respect to the C—C one ($\tau_1 = 180°$), the preference for this conformation being due to the electrostatic repulsion between the positively charged atoms H

and C (see scheme 6). Of some interest is the conformation assumed by the C_bH_2 group which at $\alpha = 110°$ is planar, and lying on the OCC plane ($\rho_b = 90°$). The rotational barrier of this group is rather modest (6.9 kcal/mole), practically the same as that obtained with standard geometrical parameters [39].

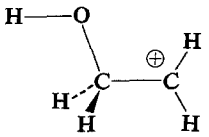

(6)

The explanation of this barrier in cations of the $XCH_2—CH_2^+$ type is generally [40, 15] given by invoking hyperconjugation between the formally empty p orbital of the methylene group and an orbital of the same symmetry on the adjacent C atom of the CH_2X group, and a differential effect due to the difference of electronegativity between the substituent X group and H. If the electronegativity of X is higher than that of H, the carbon p orbital involved in the bond with X is less available, and as a consequence the hyperconjugation prefers the eclipsed form reported in scheme 6. This explanation could be accepted for cations in their equilibrium geometry, but does not explain the torsional barrier of this group at different geometries. For instance at $\alpha = 90°$ (see Table 6) the preferred value of ρ_b is 0°. We give in Fig. 3 the rotational curves for $\alpha = 90°$ and 110°. The changes in the geometry do not permit any more the schematization of the CH_2 group as a planar methylenic group with an empty p orbital and the simple orbital interaction scheme summarized above cannot be employed.

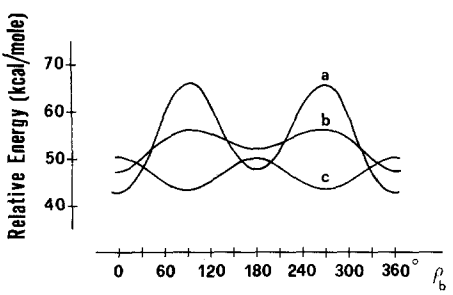

Fig. 3. Rotation of the C_bH_2 group in $HOCH_2CH_2^+$ (ρ_b angle). Curve a: $\alpha = 90°$, $\tau_1 = 104°$; curve b: $\alpha = 90°$, $\tau_1 = 180°$; curve c: $\alpha = 110°$, $\tau_1 = 180°$

The differences in the internal geometry and charge distribution of $C_2H_4OH^+$ at $\alpha = 90°$ and 110° are quite consistent, and the impression deduced from not wholly optimized calculations at intermediate α values is that this change takes place rather abruptly after the crossing of the α barrier which occurs at $\alpha \simeq 100°$ (see Fig. 2). The height of this barrier is, according to our STO-3G calculations, 45 kcal/mole. Using a larger basis set (but not an optimization of the geometry of the intermediate state), Hopkinson *et al.* [15] obtain as the lower value of the barrier 25 kcal/mole. These authors consider this value as an underestimation of the real barrier.

6. The Formation of the 2-Fluoroethanol from $C_2H_4OH^+$

An attack on the oxiranium ion in the cyclic structure performed by a negative ion X^- is easy and leads to the formation of the halohydrine without barrier and with

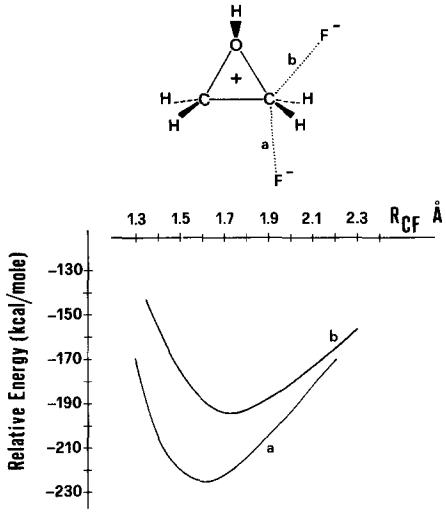

Fig. 4. Comparison of the energy profiles for the two best ways of attack of F^- on $C_2H_4OH^+$ in the ring plane. The relative energy is measured starting from the isolated reactants F^- and $C_2H_4OH^+$

a preference for the inversion of configuration. The examination of the approach paths of F^- to $C_2H_4OH^+$ (with retention of the internal geometry of this ion) shows up two cones where the approach is favoured. The minimum energy paths within these two cones are not far from the ring plane (which in $C_2H_4OH^+$ is no longer a symmetrical plane) and can be approximated by two straight lines making an angle with the C—C axis respectively of 97° and 223°.

The energy profiles along such paths are given in Fig. 4. It is evident that path *a*, corresponding to the attack on the C—C side of the ring, is favoured. The constraint of keeping rigid the internal geometry of $C_2H_4OH^+$ can be accepted only for the early stages of the reaction. The elimination of this constraint gives a description of the reaction mechanism which corresponds, for both approach paths, to a synchronous enlargement of the α angle (i.e. a lengthening of the O—C_b bond) and a change in the geometry of C_bH_2 group, with formation of fluoroethanol without any further barrier. The preference for the inversion of configuration seems to be ruled by quantitative rather than by qualitative differences in the two competitive channels.

Less easy is the formation of fluoroethanol starting from $C_2H_4OH^+$ and HF. By analogy with what was found in the case of neutral oxirane the attack of HF on the C_bH_2 group leads to the formation of an H bonded complex (F acts as proton acceptor). The opening of α angle is a little easier in this complex than in $C_2H_4OH^+$ alone: at $\alpha = 70°$ the required energy is 7 kcal/mole instead of 11.5 kcal/mole in $C_2H_4OH^+$. The passage from this H bonded complex to geometries having F directly bound to C_b is easier at larger α angles ($\alpha \simeq 90°$) and requires a more substantial increase of the potential energy, which we have not considered necessary to evaluate with care because the energy profile is nearly dominated by the energy necessary to remove the extra proton of HO—CH_2—CH_2—FH^+. This energy at $\alpha = 112°$ is 192 kcal/mole. The best reaction path for this reaction corresponds to inversion of configuration but it is clear that without the intervention of other

factors (e.g. a solvent) this reaction is not possible. This topic will be considered in the final discussion.

7. The Search for a Concerted Mechanism for the Ring Opening

We have examined in the preceding section mechanisms which assume a previous dissociation of the HF molecule. We shall pass now to examine different mechanisms where the cleavage of the F—H bond accompanies the cleavage of the O—C_b bond. The method of search for a transition state cannot be the same as that employed in the search for a minimum. We have adopted a strategy of sequential determination of provisional values for a set of geometrical parameters considered to be the most important in characterizing the mechanism. This determination has been performed with simultaneous optimization of practically all the other geometrical parameters not yet determined in the sequence and using, where possible, a procedure which we have found convenient in other analogous investigations (see e.g. Alagona *et al.* [41]). This procedure consists in determining, for the parameter p_i in question, the projection on the p_i axis of two surface cuts, the first lying on the reagents side of the hypersurface, the second on the products side. These two cuts start from the two points on the energy surface having a geometry determined in the preceding steps of the transition state search and permit the identification of a value of p_i where the two cuts have the same energy. This value of p_i is adopted as a provisional value of that coordinate at the transition state.

A sequential determination of the numerous parameters necessary to identify the transition state geometry is not however sufficient to ensure having reached a reliable description of this particular point of the configuration space. We have thus implemented this sequential determination of the parameters, with surface scans performed in appropriate subspaces, iterative refinements for some parameters, parallel sequences for different definitions of the parameters, and checks on the description of the transition state geometry we have obtained. The following description takes into account also these complementary controls and gives at the same time a rough idea of the actual steps of the mechanism.

I) Opening of the ring angle α. The provisional value of α has been obtained as the crossing of the two curves of Fig. 5.[3] Curve *a* starts from the point corresponding to the adduct (Table 4, column A) and curve *b* from the point corresponding to fluoroethanol (Table 2, column A). The actual cross occurs at $\alpha \simeq 72°$ but the values for $\alpha = 70°$, given in Table 4, column B and Table 2, column D for the two structures, can be considered representative enough of the geometry changes produced by this variation of α. The energy rise with respect to the isolated reactants is 13.4 kcal/mole.

II) Conformational changes in the C_aOH *group.* The adduct-like geometry obtained above has the H—F group oriented in a direction not favourable for a reactive interaction with C_b. This rotation around the C_a—O axis ($\tau_1 \rightarrow -60°$) requires but a moderate energy (~ 1.6 kcal/mole) and is easier at $\alpha = 70°$ than at $\alpha = 59°$.

---

[3] Unless otherwise specified we have taken as zero the energy of the species at infinite distance.

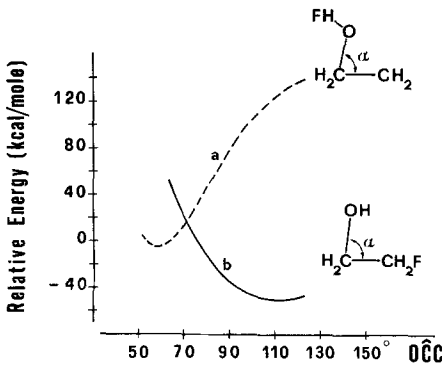

Fig. 5. Search of a preliminary guess of α in the transition state. Curve a: adduct-like geometries, curve b: fluoroethanol-like geometries. Both curves are optimized in all the parameters. The crossing of the two curves occurs at $\alpha = 72°$

III) *Changes in the* O—H *distance.* The variation of this parameter cannot any more be considered, as in the case of the preceding two, as an actual consecutive step in the reaction mechanism, but rather it represents a part of a concerted variation of a small set of parameters which correspond to the formation of the new covalent bonds H—O and C—F and the cleavage of the F—H bond. The intersection of curves given in Fig. 6 suggests a value of 1.15 Å for R_{OH}. These curves have been obtained with values of α and τ_1 kept fixed respectively at 70° and −60° and optimization of all the other parameters. Analogous curves calculated with different values of τ_1 or with optimization of τ_1 in a restricted range of values indicate the choice reported in the figure as the best candidate for the transition state.

The increase of energy corresponding to this stage of optimization is 34.9 kcal/mole.

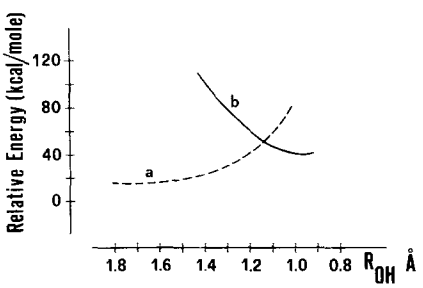

Fig. 6. Search of a preliminary guess of R_{OH} in the transition state. Curve a: adduct-like geometries ($\alpha = 70°$, $\tau_1 = -60°$); curve b: fluoroethanol-like geometries ($\alpha = 70°$, $\tau_1 = -60°$). Both curves are optimized in all the other parameters. The crossing occurs at $R_{OH} = 1.14$ Å

IV) *Orientation of* HF *with respect to the oxirane plane.* In the preceding determinations no constraints have been imposed on the dihedral angles between the planes OC_aC_b, OHC_b and OFC_b. Because the angle between these last two planes is quite small, we have preferred at this stage to make all the four atoms, O, H, F and C_b lie on the same plane, and to introduce as a new variable the dihedral angle β between the planes OC_aC_b and $OHFC_b$. We have performed parallel determinations of the following parameters in the sequence with three different values of β (i.e. 180°, 150° and 120°). The last value being the closest to the final value of β (see point *VIII*) we report here the results obtained with this choice of the dihedral angle (energy increase 13.8 kcal/mole).

V–VI) *Changes in the orientation of* HF (*angle* $\widehat{OHF}$) *and in the* R_{HF} *distance.* With the values of the parameters already determined we have selected for $\widehat{OHF}$ the

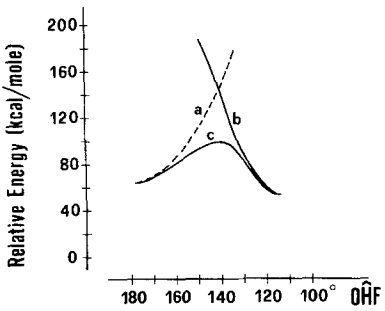

Fig. 7. Search of a preliminary guess of $\widehat{OHF}$ and R_{HF} in the transition state. Curve a: adduct-like geometries ($\alpha = 70°$, $\tau_1 = -60°$, OH = 1.15 Å, $\beta = 120°$); curve b: fluoroethanol-like geometries ($\alpha = 70°$, $\tau_1 = -60°$, OH = 1.15 Å, $\beta = 120°$). The crossing occurs at $\widehat{OHF} = 141°$. Curve c shows the energy variations for changes in $\widehat{OHF}$ obtained by adopting the values of α, τ_1, OH, β, and $\widehat{OHF}$ reported above and by optimizing at each value of $\widehat{OHF}$ all the other parameters. In this final case the two curves corresponding to the adduct-like and to the fluoroethanol-like geometries coincide at the top of barrier ($\widehat{OHF} = 140°$, HF = 1.048 Å and the remaining parameters as given in column V of Table 7)

value of 140° by means of the two curves given in Fig. 7. These two curves have again been obtained with optimization of all the remaining parameters.

At this stage one can pass to a direct optimization of the last parameter (R_{HF}) necessary to define the geometry of the $OHFC_b$ group (the other four being α, τ_1, R_{OH} and $\widehat{OHF}$). The result of this optimization is reported as curve *c* in Fig. 7. The best value of R_{HF} is of 1.048 Å. The changes of the $\widehat{OHF}$ angle and of the HF distance correspond to an energy rise of 35.7 kcal/mole.

This sequential determination of the transition state geometry gives an energy barrier of 99.4 kcal/mole.

In Table 7 we list the geometry variations in this sequence of determinations, starting from the $C_2H_4O \cdot HF$ adduct given in Table 4 up to this provisional definition of the transition state.

VII) *A further refinement of the most favourable geometry* for the reaction at $\alpha = 70°$ and $\beta = 120°$ has been obtained with a different definition of the parameters describing the reciprocal arrangement of the four atoms $OHFC_b$. The most noticeable difference is in the value of the $\widehat{C_bOH}$ angle and of the CF distances which pass respectively from 75° to 70° and from 1.8 to 1.66 Å, with a decrease of the energy of 2.6 kcal/mole.

VIII) *Search for the best dihedral angle.* A parallel investigation, with fixed values of α and R_{OH} has been performed at some other values of β (viz. 180°, 150°, 130°, 97°). The results are shown in Fig. 8. It appears that for a wide range of β (from 120° to 240°) the energy barrier does not change by more than 10 kcal/mole. The best value of β is about 124° ($\Delta E \simeq 93$ kcal/mole).

Table 7. Changes of the most important parameters[a] in the course of the sequential determination of the transition state for the concerted reaction with retention of configuration[b]

	I	*II*	*III*	*IV*	*V*
$\widehat{OC_aC_b}$ (α)	*70*[d]	*70*	*70*	*70*	*70*
τ_1	−104.0	*−60*	*−60*	*−60*	*−60*
OH	1.754	1.790	*1.150*	*1.150*	*1.150*
C_aC_bOH	109.21	147.51	152.04	*120*	*120*
C_aC_bOF	107.62	147.25	152.76	*120*	*120*
$\widehat{OHF}$	174.00	174.00	181.00	178.00	140.00
HF	0.955	0.955	1.008	1.023	1.048
$\widehat{C_bOH}$	116.95	101.06	105.78	76.09	75.16
$\widehat{HFC_b}$	26.17	31.87	30.35	43.00	73.40
C_bF	3.692	3.390	3.028	2.359	1.809
C_bO	1.607	1.610	1.609	1.631	1.727
C_aO	1.386	1.387	1.398	1.435	1.486
C_aC_b	1.415	1.420	1.410	1.410	1.525
$\widehat{C_aC_br_b}$	165.60	165.60	168.00	170.00	141.10
E, hartrees	−249.48001	−249.47745	−249.42181	−249.39989	−249.34298
ΔE,[c] kcal/mole	13.4	15.0	49.9	63.7	99.4

[a] Distances in Å, angles in degrees.

[b] The columns are numbered according to the sequential steps described in paragraph 7. The geometries refer to points lying on the reactant side of the hypersurface.

[c] The energy differences are given with respect to the separate reagents. $E(C_2H_4O) + E(HF) = -249.50315$ hartrees.

[d] The values in italics are not optimized.

IX) Checks on the planarity of the $OHFC_b$ *group.* There are no theoretical reasons to suppose that the four atoms must lie exactly on the same plane. Checks performed at $\beta = 120°$ indicate that the actual dihedral angle between the OHC_b and the OFC_b planes is not larger than 5–7 degrees. The elimination of this constraint corresponds to a lowering of the energy barrier of about 1.5 kcal/mole.

X) Checks on the value of the α *angle.* The value of the ring opening angle was fixed at the very beginning of this investigation. To check if the provisional value $\alpha = 70°$ adopted for this investigation was sufficiently near the actual value of α at the top of the barrier, we have performed a partial optimization of the parameters (steps *II–VII* of this procedure) for $\alpha = 60°$, 80° and 90°. The energies obtained with these optimizations are reported in Fig. 9. It appears that the best value of α is close to 73°.

To conclude, the point nearest to the top of the barrier we have obtained with the present investigation has the following set of characterizing parameters (all values rounded off): $\alpha = 73°$, $\beta = 124°$, $R_{C_bO} = 1.8$ Å, $R_{OH} = 1.15$ Å, $R_{HF} = 1.05$ Å, $R_{CF} = 1.59$ Å, $\widehat{C_bOH} = 63°$, $\widehat{OHF} = 147°$, $\widehat{HFC_b} = 73°$, $\widehat{FC_bO} = 77°$, $\rho_b = 31°$ and $\widehat{C_aC_br_b} = 141°$. The corresponding energy increase (with respect to C_2H_4O + HF) is 89.7 kcal/mole. This point on the nuclear configuration space does not correspond of course to the actual transition state, but it may be considered representative enough of its geometry.

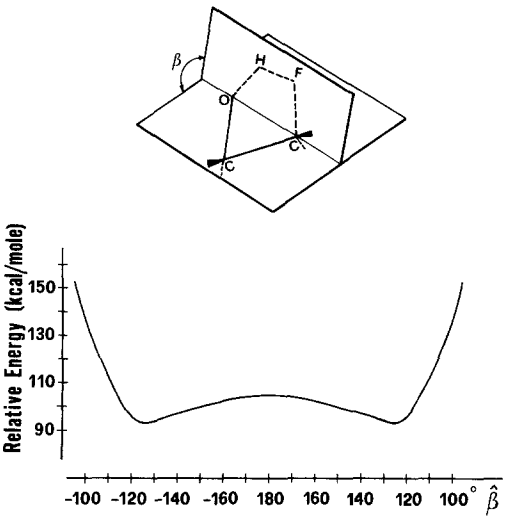

Fig. 8. Variation of the barrier energy at different values of β

8. Retention versus Inversion of Configuration

It must be observed that the set of parameters chosen for the sequential determination of the characteristics of the transition state geometry did not comprise a pair of parameters directly related to the configuration assumed by the final product (i.e. ρ_b and $\widehat{C_aC_br_b}$). These two parameters have been subjected to optimization at each step of the procedure outlined above, and the results show (see Table 8) that the reaction mechanism we have identified corresponds to retention of configuration.

The alternative mechanism leading to the inversion has, for the physical model under examination, a decidedly higher energy barrier and requires more stringent initial conditions than the retention mechanism.

To get a description of the transition state and of the reaction coordinate for inversion we have been compelled to resort to a systematic search of initial conditions and of subsequent geometry rearrangements which do not lead in the end to retention.

A previous opening of C_2H_4O ($\alpha \simeq 80$–$90°$) and an attack of HF on the C_b atom constitute the best initial conditions. As we have remarked in a preceding section,

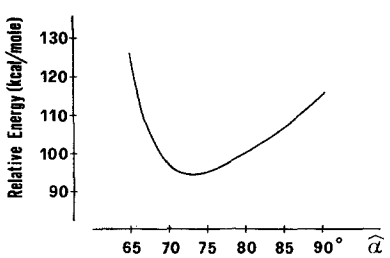

Fig. 9. Variation of the barrier energy at different values of α

Table 8. Comparison of the essential parameters of the approximate description of the transition state geometries for the retention and inversion reactions

	A	B
Angles, deg		
α	70	80
β	120	90
$\widehat{C_bOH}$	75.2	63.0
$\widehat{OHF}$	140.0	141.9
$\widehat{HFC_b}$	73.4	70.0
$\widehat{FC_bO}$	71.4	85.0
ρ_b	31.8	−45.0
$\widehat{C_aC_br_b}$	141.1	203.4
Distances, Å		
C_bO	1.73	1.80
OH	1.15	1.51
HF	1.05	1.05
C_bF	1.81	1.80

A: retention of configuration.
B: inversion of configuration.

when the α angle of oxirane is between 80° and 90° an inversion of the C_b atom occurs spontaneously (for $\alpha = 70°$ the inversion mechanism is not possible). At the same time the best direction of attack of HF (with F pointing towards C_b) on this distorted oxirane roughly corresponds to the bisector of $\widehat{C_aC_br_b}$ (see Sect. 6 for analogous attacks). The best initial conditions for inversion are in fact given by an attack on C_2H_4O having $\alpha \simeq 85°$, along an approach path having $\widehat{C_aC_bF} \simeq 95°$ and $\widehat{C_bFH} = 180°$. The next portion of the reaction path corresponds to a rotation of the $CH_2 \cdots FH$ group which brings HF into a plane nearly perpendicular to the ring. FH is only loosely bond to CH_2 and the values assumed by the rotational angles OC_aC_bF (τ_2) and $OC_aC_br_b$ (ρ_b) (this last defines the rotation of C_bH_2 around the C_aC_b axis) are not the same. When τ_2 is equal to 0°, 45° and 90°, ρ_b assumes respectively the values 0°, 18° and 45°. A further step in the reaction consists in a bending of the HF group on the plane containing also the C_b and O atoms ($\beta = 90°$) and in a simultaneous reduction of the $\widehat{OC_bF}$ angle. To obtain the definition of the reaction path we have spanned a portion of the three-dimensional subspace defined by these two angles and by R_{CF} ($180° \geqslant \widehat{C_bFH} > 70°$; $110° \geqslant \widehat{OC_bF} \geqslant 60°$; $2.1 \geqslant R_{CF} > 1.7$). The value $R_{CF} = 1.8$ Å has been verified to be the most suitable to get the inversion transition state.

The values assumed by $\widehat{C_bFH}$, $\widehat{OC_bF}$ and R_{CF} are rather critical because when C_aC_bFH is near 90° it is quite easy to pass to a retention reaction path. It has been necessary to verify for each combination of these parameters whether or not the corresponding point on the nuclear configuration space actually lies in the region of the inversion path. This control has been made by examining in every case the energy profile for changes in ρ_b. We give in Fig. 10 simply as an example the energy

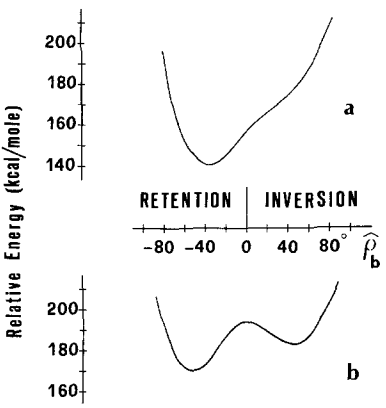

Fig. 10. Two examples of changes in energy for rotations of C_bH_2 around the C_a—C_b axis (ρ_b angle). Curve a: $\widehat{OC_bF} = 78.3°$; curve b: $\widehat{OC_bF} = 90°$. Both curves are calculated with $\widehat{C_bFH} = 180°$, CF = 1.8 Å and $\beta = 90°$; the values of the other parameters as specified in the text

curves for changes in ρ_b for the two cases differing only in the $\widehat{OC_bF}$ angle (78.3° in Fig. 10a and 90° in Fig. 10b). The analysis of the results we have obtained shows that the inversion path is contained in a rather narrow valley of the subspace of the angular C_aC_bFH and $\widehat{OC_bF}$ coordinates with values near 90 degrees for both of them.

We have reached a geometrical configuration having the four atoms $OHFC_b$ on the same plane ($\beta = 90°$). When $R_{HF} = 1.05$ Å this configuration corresponds to the point nearest to the transition state we have detected. The whole energy barrier is of the order of 185 kcal/mole. Its dissection gives 50 kcal/mole for the opening of oxirane, 30 for the attack of HF ($R_{CF} = 1.8$ Å), 60 for the rotation of the CH_2—FH group, 45 for the final arrangements in the C_bFHO plane (of which around 20 for

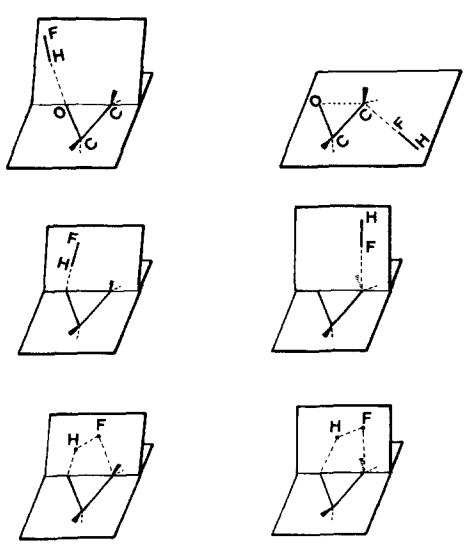

Fig. 11. Comparative schematic picture of the two reaction paths until the transition state. On the left the retention path, on the right the inversion path

the elongation of the HF bond and around 20 for the bending of the HF group). All these values are rounded off.

This description of the transition state is less refined than that done for the retention transition state (refinement steps corresponding to points *VII–X* of the preceding section are lacking) but it seems sufficient to us to establish that the inversion reaction in C_2H_4O + HF, via a concerted mechanism, is much more difficult than the retention one.

We give in Fig. 11 a comparative schematic picture of the two reaction paths and we report in Table 8 the geometrical parameters identifying the approximation to both the transition states obtained at the same level of refinement. It is evident that the inversion mechanism requires a larger value of $\widehat{OC_bF}$, and of consequence larger values for either the distance R_{OH} or R_{CF} (the range of possible variations of HF is quite small). The method of searching the transition state we have followed perhaps favours R_{CF}, and R_{OH} has turned out decidedly longer than in the retention mechanism. With a different strategy one could perhaps arrive at a somewhat lower R_{OH}/R_{CF} ratio, but without much affecting, in our opinion, the value of the barrier height.

The numerical estimates of the energy barriers we have reported above represent an overestimate of their actual values because of the smallness of the basis set and of the possible inadequacy of the one-determinant approximation in describing electronic structures with distorted and stretched bonds. To get an estimate of these effects we have repeated the SCF calculations for the reagents and for the geometrical structures reported in Table 8 with the 4-31G basis set, obtaining the following values of the energy differences between reagents and transition-like geometries: ΔE(ret) = 84 kcal/mole, ΔE(inv) = 141.7 kcal/mole. It should be remembered that a further improvement in the STO-3G SCF description of the retention barrier has led to a lowering of 9.7 kcal/mole in the barrier height (from 99.4 to 89.7 kcal/mole, see Sect. 7), and presumably an analogous lowering should be also present in the 4-31G SCF approximation.

At the same time we have performed with the STO-3G basis set a few CI calculations for the geometries of Table 8, for the reagents and for the $C_2H_4O \cdot HF$ adduct. These calculations have been performed by successive diagonalizations of secular matrices having an increasing number of configurations (from 3 to 16) and by estimating with a second-order perturbative calculation the effects of a larger number of determinants ($\sim$180,000) not directly included in the diagonalization procedure. For these calculations we have employed the CIPSI program [42]. The calculations with a small number of configurations permitted us to verify that near the transition state the electronic configuration given by the SCF procedure is actually the dominant one, while the larger calculations (with inclusion of the second order contributions) give a better estimation of the energy barriers in the STO-3G basis set. The relative weight of the most important configurations is reported in Table 9. The CI calculations produce a lowering of $\sim$32 kcal/mole in the retention barrier (from 99.4 to 67.5 kcal/mole) and $\sim$48.5 for the inversion one (from 185 to 136.6 kcal/mole). Taking into account again the improvements on the

Table 9. Relative weights of the most important configurations in the CI calculations on thes tructures A and B of Table 8. Single and double excitations are indicated by one or two hole-particle couples.

A		B	
SCF ground state	0.95901	SCF ground state	0.86475
(16, 18) (17, 25)	0.01863[a]	(17, 18) (17, 18)	0.09675
	0.00739[b]	(17, 18)	0.01828
(17, 18) (17, 18)	0.01488	(14, 18) (17, 18)	0.00850
(13, 18) (13, 18)	0.00882	(15, 18) (17, 18)	0.00750
(13, 18)	0.00509	(14, 18)	0.00422
(15, 19) (15, 19)	0.00199		

[a] This weight refers to the configuration: $\frac{1}{2}[\alpha\beta\alpha\beta - \beta\alpha\alpha\beta - \alpha\beta\beta\alpha + \beta\alpha\beta\alpha]$.
[b] This weight refers to the configuration:
$1/\sqrt{3}\{\beta\beta\alpha\alpha - \frac{1}{2}[\alpha\beta\alpha\beta + \beta\alpha\alpha\beta + \alpha\beta\beta\alpha + \beta\alpha\beta\alpha] + \alpha\alpha\beta\beta\}$.

description of the transition state we have performed after these calculations we may consider a value of ~60–55 kcal/mole as a reliable estimate of the retention barrier in the STO-3G basis set.

9. Discussion and Conclusions

The different mechanisms we have examined give partial but supplementary information on the reaction under examination.

Under gas phase conditions the reaction proceeds through a concerted non-ionic mechanism. As we have seen above the reaction is aided by the formation of a hydrogen bonded complex. The following stage of the reaction corresponds to a weakening of the O—C bond (in oxirane of course there are two symmetrical reaction paths involving one of the two C—O bonds) and to internal rotations in the $C_2H_4O \cdot HF$ complex. The next portion of the reaction path corresponds to the concerted formation of the two new covalent bonds O—H and C—F and cleavage of F—H bond. The motion of the C_bH_2 group during this process roughly corresponds to a rotation of this group around the C_a—C_b axis (ρ_b passes from 0° to ~32°) and the whole mechanism corresponds to a retention of configuration.

More exacting are the conditions corresponding to an inversion mechanism. The formation of an H bonded complex does not favour this particular mechanism and only a direct approach of HF to the CH_2 group in a plane perpendicular to the ring ($\beta \simeq 90°$) can lead to inversion at the C_b atom. In this case the motion of the C_bH_2 group is better described as an inversion ($\widehat{C_aC_br_b}$ passes from 155° to 203°).

Also the heights of the energy barriers indicate as more probable the reaction with retention. In this case the barrier is estimated to be below 60 kcal/mole, while for the inversion mechanism we have calculated as an upper limit to the barrier 135 kcal/mole.

The application of this description of the mechanism to other analogous gas phase reactions should be made with some precautions. In fact, apart from the occurrence of other factors of electronic and steric origin deriving from a substitution of H atoms of the epoxidic substrate with other groups, whose effect greatly depends on the nature of the substituent, even the simple substitution of HF with another halogenic acid may modify the energy profiles of the two reactions. HCl and HBr have a lower dissociation energy and a larger bond length than HF, and one may safely presume that these changes reduce the barrier heights. In addition, if the hydrogen halide had a larger bond length, the conditions for the inversion path should be less stringent, and of consequence for HCl and HBr the barrier heights of the two mechanisms could be more comparable.

The other reaction mechanisms are not favoured in the gaseous phase because the dominant contribution to the barrier height is given in those cases by the ionic dissociation of the H—F bond (experimentally $\sim$370 kcal/mole). The situation could, however, be completely different in solution.

As we remarked in the introduction, in really anhydrous inert solutions of HX there is no appreciable concentration of free ions. There remains however the possibility that the interaction of HX with the epoxide produces, via the formation of a H bonded complex, the formation of ions (i.e. X^- and the conjugate acid of the epoxide) although conductometric measurements performed during the reaction do not evidence a great rise of the conductivity.

Experimental and computational data at our disposal are not suitable for giving an estimate of the free energy change in this heterolytic cleavage, but are sufficient to infer that, if this cleavage occurs, the separation of the ions is probably not complete and X^- remains loosely bound to the conjugate acid of the epoxide until the formation of halohydrine occurs (see Sect. 6). This reaction should occur via an A_2 mechanism with inversion of configuration.

Still retaining the assumption of the formation of $C_2H_4OH^+$, the calculations do not indicate as favoured the reaction with a neutral HF molecule. The A_1 mechanism requires the passage of a barrier due to the opening of the $C_2H_4OH^+$ cation which according to the best available calculations is of the order of more than 25 kcal/mole [15] and which presumably will not be reduced noticeably by solvent effects. The A_2 mechanism is discarded by the calculations, while a "borderline A_2" mechanism could be possible if the solvent effect reduces the energy required for the heterolytic cleavage $HOCH_2CH_2FH^+ \rightarrow HOCH_2CH_2F + H^+$. In this case too there remains an energy barrier not present in the reaction $C_2H_4OH^+ + X^-$.

In all cases mechanisms requiring as a primary step the protonation of oxirane should lead to solutions containing noticeable amounts of free ions which are not evident in conductometric measurements of really anhydrous solutions.

We have previously remarked that the gas phase barriers should have become lower if one had used other reagents instead of HF. We may add that even in solutions of HF there is another possibility of noticeably reducing the barrier heights.

If the concentration of HF is high enough, a part of this reagent will be present in the form of dimers: HF·HF. We have shown in a previous paper [38] that dimeric association enhances the reactivity of HF (both as electrophile and as nucleophile) and greatly reduces the energy necessary for the heterolytic cleavage of H—F. We have also remarked in a preceding section of this paper that a noticeable contribution to the two concerted reaction barriers derives from geometry constraint imposed by the smallness of the HF bond length. If HF·HF were the actual reactant these geometry constraints should be greatly reduced with a consequent reduction of the barrier heights (especially for the inversion mechanism). A similar hypothesis has been tentatively considered in a recent paper on the kinetics of the reactions of epoxides with HCl in low polarity aprotic solvents [9], but the difficulty of getting reliable data has not permitted to verify it. In fact precise experimental results for reactions performed in "inert" solvents are at present scarce and apparently contradictory (see, for a concise and clear summary, Ref. [9]) and more accurate determinations of the true rate constants are needed before reaching a satisfactory interpretation of the reaction mechanism in these solvents. It may be remarked, as a further suggestion, that the occurrence of the very small amount of water, which presumably is present also in anhydrous inert solvents, could be of some effect on the reaction barrier and reaction rate, via the formation of adducts $H_2O \cdot HX$ [38].

In conclusion, although our calculations give too high an estimate of the barriers for the concerted mechanisms, there are sufficient reasons to consider that the concerted mechanism which rules the gas phase reaction could be a possible candidate even for the reaction in solution.

References

1. Parker, R. E., Isaacs, N. S.: Chem. Rev. **59**, 737 (1959)
2. Biggs, J., Chapman, N. B., Finch, A. F., Wray, V.: J. Chem. Soc. (B) 55 (1971); Biggs, J., Chapman, N. B., Wray, V.: J. Chem. Soc. (B) 63, 66, 71 (1971)
3. Buchanan, J. G., Sable, H. Z., in: Selective organic transformations, Vol. 2, p. 1, Thyagarajan, B. S. ed. New York: Wiley-Interscience 1972
4. Pritchard, J. G., Siddiqui, I. A.: J. Chem. Soc. Perkin II 452 (1973)
5. Carr, M. D., Stevenson, C. D.: J. Chem. Soc. Perkin II 581 (1973)
6. Kakuchi, H., Iijima, T.: Bull. Chem. Soc. Japan **46**, 1568 (1973)
7. Wohl, R. A.: Chimia **28**, 1 (1974)
8. Lamaty, G., Malog, R., Selve, C., Sivade, A., Wylde, J.: J. Chem. Soc. Perkin II 1119 (1975)
9. Bellucci, G., Berti, G., Ingrosso, G., Vatteroni, A., Ambrosetti, R., Conti, G.: J. Chem. Soc. Perkin II 627 (1978)
10. Hayes, E. F.: J. Chem. Phys. **51**, 4787 (1969)
11. Hayes, E. F., Siu, A. K. Q.: J. Am. Chem. Soc. **93**, 2090 (1971)
12. Mezey, P., Kari, R. E., Denes, A. S., Csizmadia, I. G., Gosavi, R. K., Strausz, O. P.: Theoret. Chim. Acta (Berl.) **36**, 329 (1972)
13. Fujimoto, H., Katata, M., Yamabe, S., Fukui, K.: Bull. Chem. Soc. Japan **45**, 1320 (1972)
14. Frenking, G., Kato, H., Fukui, K.: Bull. Chem. Soc. Japan **48**, 6 (1975)
15. Hopkinson, A. C., Lien, M. H., Csizmadia, I. G., Yates, K.: Theoret. Chim. Acta (Berl.) **47**, 97 (1978)
16. Bonaccorsi, R., Scrocco, E., Tomasi, J.: J. Am. Chem. Soc. **52**, 5270 (1970)
17. Petrongolo, C., Tomasi, J.: Chem. Phys. Letters **20**, 201 (1973)
18. Ghio, C., Tomasi, J.: Theoret. Chim. Acta (Berl.) **30**, 151 (1973)

19. Catalán, J., Yáñez, M.: J. Am. Chem. Soc. **100**, 1398 (1978)
20. Alagona, G., Cimiraglia, R., Scrocco, E., Tomasi, J.: Theoret. Chim. Acta (Berl.) **25**, 103 (1972)
21. Bonaccorsi, R., Cimiraglia, R., Scrocco, E., Tomasi, J.: Theoret. Chim. Acta (Berl.) **33**, 97 (1974)
22. Eisenstein, O., Lefour, J. M., Minot, C.: Tetrahedron Letters **20**, 1681 (1976)
23. Lathan, W. A., Radom, L., Hariharan, P. C., Hehre, W. J., Pople, J. A.: Topics Curr. Chem. **40**, 1 (1973)
24. Gunde, R., Azman, A.: J. Mol. Struct. **27**, 212 (1975)
25. Buckton, K. S., Azrak, R. G.: J. Chem. Phys. **52**, 5652 (1970)
26. Hagen, K., Hedberg, K.: J. Am. Chem. Soc. **95**, 8263 (1973)
27. Radom, L., Lathan, W. A., Hehre, W. J., Pople, J. A.: J. Am. Chem. Soc. **95**, 693 (1973)
28. Pople, J. A., Radom, L., in: Conformation of biological molecules and polymers, Jerusalem Symposia, vol. V, 747 (1973)
29. JANAF thermochemical Tables, D. R. Stull, ed. Midland, Mich.: Dow Chemical 1965
30. Rossini, F. D., Wagmam, D. D., Evans, W. H., Levine, S., Jaffe, I.: Natl. Bur. of Standards Circ. No. 500. Washington, D.C. 1952
31. Wyn-Jones, E., Orville-Thomas, W. J.: J. Mol. Struct. **1**, 79 (1968)
32. Cimiraglia, R., Persico, M., Tomasi, J.: Chem. Phys. **24**, 51 (1977)
33. Nesbet, R. K.: Rev. Mod. Phys. **35**, 552 (1963)
34. Dewar, M. J. S., Hashmall, J. A., Venier, C. J.: J. Am. Chem. Soc. **90**, 1953 (1968)
35. Salem, L.: J. Am. Chem. Soc. **96**, 3486 (1974)
36. Segal, G. A.: J. Am. Chem. Soc. **96**, 7892 (1974)
37. Horsley, J. A., Jean, Y., Moser, C., Salem, L., Stevens, R. M., Wright, J. S.: J. Am. Chem. Soc. **94**, 279 (1972)
38. Alagona, G., Scrocco, E., Tomasi, J.: Theoret. Chim. Acta (Berl.) **47**, 133 (1978)
39. Radom, L., Pople, J. A., Schleyer, P. v. R.: J. Am. Chem. Soc. **94**, 5935 (1972)
40. Hoffmann, R., Radom, L., Pople, J. A., Schleyer, P. v. R., Hehre, W. J., Salem, J.: J. Am. Chem. Soc. **94**, 6221 (1972)
41. Alagona, G., Scrocco, E., Tomasi, J.: J. Am. Chem. Soc. **97**, 6976 (1975)
42. Huron, B., Malrieu, J. P., Rancurel, P.: J. Chem. Phys. **58**, 5745 (1973)

Received June 21, 1978/September 25, 1978